42214 layered Fe-based superconductors: An *ab initio* study of their structural, magnetic, and electronic properties

F. Bucci,[1] A. Sanna,[2] A. Continenza,[1] S. Katrych,[3] J. Karpinski,[3] E. K. U. Gross,[2] and G. Profeta[4]
[1]*Department of Physical and Chemical Sciences, Università di L'Aquila, 67010 Coppito (L'Aquila), Italy*
[2]*Max-Planck-Institut für Mikrostrukturphysik, Weinberg 2, D-06120 Halle, Germany*
[3]*Institute of Condensed Matter Physics, EPFL, CH-1015 Lausanne, Switzerland*
[4]*Department of Physical and Chemical Sciences and SPIN-CNR, Università di L'Aquila, 67010 Coppito (L'Aquila), Italy*
(Received 4 August 2015; revised manuscript received 4 December 2015; published 25 January 2016)

As a follow-up to the discovery of a new family of Fe-based superconductors, namely, the $RE_4Fe_2As_2Te_{1-x}O_4$ (42214) (RE = Pr, Sm, and Gd), we present a detailed *ab initio* study of these compounds highlighting the role of rare-earth (RE) atoms, external pressure, and Te content on their physical properties. Modifications of the structural, magnetic, and electronic properties of the pure (e.g., $x = 0.0$) 42214 compounds and their possible correlations with the observed superconducting properties are calculated and discussed. The careful analysis of the results obtained shows that (i) changing the RE atoms allows one to tune the internal pressure acting on the As height with respect to the Fe planes; (ii) similarly to other Fe pnictides, the 42214 pure compounds show an antiferromagnetic-stripe magnetic ground state phase joined by an orthorhombic distortion (not experimentally found yet); (iii) smaller RE atoms increase the magnetic instability of the compounds possibly favoring the onset of the superconducting state; (iv) external pressure induces the vanishing of the magnetic order with a transition to the tetragonal phase and can be a possible experimental route towards higher superconducting critical temperature (T_c); and (v) Te vacancies act on the structural parameters, changing the As height and affecting the stability of the magnetic phase.

DOI: 10.1103/PhysRevB.93.024518

I. INTRODUCTION

The discovery of superconductivity in $LaFeAsO_{1-y}F_y$ belonging to the so-called 1111 family has stimulated an active search for new Fe-based compounds that, in recent years, disclosed a large variety of material families, all of them sharing similar building blocks: the prototype 1111 family has been shortly joined by the 122 (XFe_2As_2, X = Ca, Sr, Ba, K, Rb, and Cs) and the 11 compounds (FeX, X = Se and Te). Pure and stoichiometric compounds belonging to any of these families are nonsuperconductors (FeSe seems to be the only exception at the moment [1]); however, acting on doping, pressure, or vacancies a superconducting phase can be induced, with critical temperatures reaching pretty high values ($T_c \simeq$ 50–60 K [2]). Building on these previous works, Katrych and co-workers recently synthesized a new family of Fe-based superconductors, the so-called 42214 family: $RE_4Fe_2As_2Te_{1-x}O_4$, RE being a rare-earth (RE) element RE = Pr, Sm, and Gd and x being the percentage of native tellurium vacancies [3,4]. The superconducting critical temperature can be increased up to 45 K, appropriately varying the rare-earth atoms, the Te concentration, and the content of substitutional fluorine atoms on O sites [4]. Although these new compounds seem to share the same building blocks of the 1111 materials, namely, FeAs planes intercalated by RE-O layers, the presence of tellurium spacer planes adds new possibilities to modify the structural properties and the charge density of the material.

Moreover, due to the Te intercalation, the vertical distance between FeAs planes is strongly increased with respect to 1111 compounds, reaching values close to 16 Å. This makes the 42214 compounds interesting materials to possibly show intrinsic Josephson junctions (iJJ). Indeed, these last compounds can be seen as natural heterostructures of superconducting FeAs planes incorporated in a matrix of insulating layers. The small out-of-plane coherence length compared to the c-lattice spacing, makes 42214 materials particularly suitable to observe iJJ [5]. Finally, the possibility to increase the spacing between superconducting FeAs layers can represent a route to drive these systems towards hopefully higher T_c, as in the case of $Bi_2Sr_2Ca_{n-1}Cu_nO_{2n+2+x}$ for the cuprates, which brought the critical temperature over 120 K.

However, in order to fully optimize the physical properties of this new class of materials it is fundamental to ascertain the role of Te and RE-O spacing layers in determining the structure, the magnetic phase, and the electronic properties. To this end, we carried out a detailed *ab initio* study of the structural, magnetic, and electronic properties of the 42214 stoichiometric compounds (e.g., $x = 0.0$) as a function of the RE involved and, in addition, we extended the study to predict high pressure effects to trace a possible experimental route towards higher T_c. Based on the careful comparison with available experiments, we anticipate that *ab initio* results give a reliable representation of the real materials; moreover, analyzing properties of the compounds such as As height, magnetic stability, and electronic states at the Fermi level we are able to draw a consistent picture of this family and to give predictions on how to improve the material properties.

In the following, we will discuss first-principles results of the pure Pr, Sm, and Gd-based compounds and discuss their structural and magnetic properties at equilibrium (Sec. III) and under applied pressure (Sec. IV) together with their electronic properties (Sec. V). We will then discuss the reproducibility of the experimental 42214's structural parameters (Sec. VI), introducing Te vacancies through the use of supercells, and finally draw our conclusions (Sec. VII).

II. COMPUTATIONAL DETAILS

The calculations are performed using the VASP [6,7] package within the generalized gradient approximation [8] (GGA) to density functional theory, and projected augmented-wave (PAW) [9] pseudopotentials. f electrons of the RE atoms are considered as part of the core. Convergence of the relaxed structural parameters was reached using 550 eV as energy cutoff. Integration of the irreducible Brillouin zone was performed considering shells up to (14, 14, 2) within the Monkhorst and Pack scheme [10]. The presence of Te vacancies was studied using supercells containing up to 52 atoms. All the structures considered were fully relaxed following the *ab initio* calculated forces, and optimizing the cell shape to make the stress tensor vanish (up to 0.2 kbar). Fermi surfaces and nesting functions were calculated on much larger grids (64, 64, 1) and interpolated up to (400, 400, 20) points in the Brillouin zone.

III. STRUCTURAL PROPERTIES

Before starting the discussion of our first-principles results, we first analyze the experiments available to draw some preliminary conclusions.

The most general chemical formula describing this family is $RE_4Fe_2As_2Te_{1-x}O_{4-y}F_y$ and at $x = y = 0.0$ can be also described by a body-centered tetragonal (bct) crystal structure with $I4/mmm$ space group with one FeAs plane/unit cell. In the tetragonal crystal structure (see Fig. 1) there are two Fe-As planes/unit cell, oriented in opposite directions, spaced by a RE_2-O_2 plane and a Te plane with occupancy experimentally always lower than 1 (see Fig. 1). As in the other 1111 and 122 families, the unit cell is a tetragonal cell in the high temperature in the paramagnetic phase. At the moment, there are no experimental measurements at low temperature to ascertain whether the 42214 compounds undergo a structural and/or magnetic phase transition, as many of the other Fe-based superconductors. A detailed analysis of the experimental parameters determined through x-ray diffraction [4] shows a dependence of the crystal structure parameters on the RE covalent radius (R) ($R = 1.61$, 1.62, and 1.65 Å for Gd, Sm, and Pr, respectively [4]) and in more detail that (i) the lattice parameters a,c linearly grow as a function of R, (ii) the RE-O planes width linearly increases with R, and (iii) the Fe-As planes thickness linearly decreases with R. Interestingly the Gd-based compound shows an As height, $h_{As} = 1.366$ Å close to the *optimal* value for superconductivity ($h_{As} \simeq 1.38$ Å [11]); in fact, reduction of the RE covalent radius (from Pr to Gd) induces in-plane compression on the $FeAs_4$ tetrahedra which, in order to keep the Fe-As bond length constant, modifies the Fe-As-Fe bond angles leading to an increase of the As height with respect to the Fe planes.

However, these bare structural modifications caused by different RE atoms are not enough to sensibly raise the critical temperature which results to be nearly constant ($T_c \simeq 25$ K) for RE = Pr, Sm, and Gd at approximately similar Te-vacancies (x) concentration ($x \simeq 88\%$, 92%, and 90% for Pr, Sm, and Gd, respectively; see Table I of Ref. [4]). As shown by Katrych and co-workers [4], fluorine doping at oxygen sites is necessary to raise the critical temperature up to 45 (40) K in the case of RE = Gd (Sm). This is particularly evident for the Gd-based compound: at almost fixed Te-vacancies concentration, F doping increases T_c from 25 K ($x = 0.1$, $y = 0.0$) to 45 K ($x = 0.08$, $y = 0.2$), causing only a contraction of the RE-O layer thickness (up to 2%) with a negligible modification of the lattice parameters a and c [4].

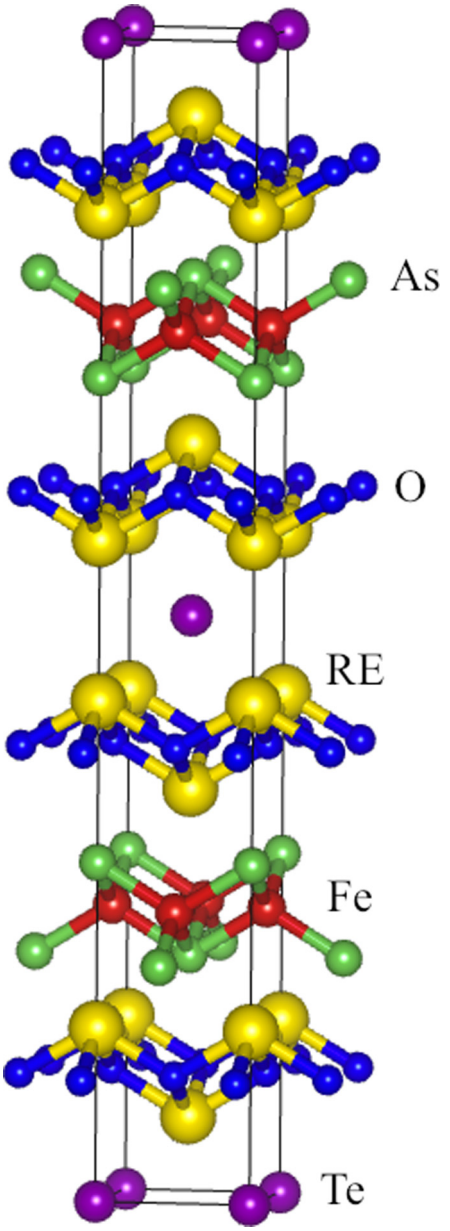

FIG. 1. Crystal structure of the 42214 compounds: 3D view of the tetragonal cell. Here red, green, yellow, blue, and purple circles represent Fe, As, RE, O, and Te atoms, respectively.

The effect of Te vacancies is even more subtle. Experiments allow comparison between two samples of the Sm-based compound: undoped ($y = 0.0$) with 92% Te content, and F doped ($y = 0.3$) with only 72% Te content. Assuming that F doping should not bring major structural effects on the lattice parameters, as found in the Gd-based compound, the comparison of the structural properties shows that the effect of increasing Te vacancies produces a contraction of the

parameters a and c (lower than 1%) and changes up to 3% the distances between the various planes.

To summarize: (i) substitution of the RE atom induces the larger changes for the lattice and internal structural parameters but seems to only marginally affect the critical temperature; (ii) Te vacancies and F doping seem to both increase the critical temperature with marginal implications on the 42214 structures.

However, the previous analysis based only on experimental results is not conclusive and does not allow one to disentangle the effects of Te vacancies and F doping or to understand if there is room to possibly further increase the superconducting transition temperature. First-principles calculations will help to understand the interplay between structural, magnetic, and electronic properties and their possible correlations with the critical superconducting temperature (T_c).

In order to predict the ground-state phases of various compounds, we performed total energy calculations, fully relaxing volume, lattice parameters, and internal positions, considering the nonmagnetic phase and two possible antiferromagnetic arrangements: the checkerboard phase (AFM1) with antiparallel Fe spins along both the in-plane axes, and the so-called stripe phase (AFM2) with Fe moments parallel along the in-plane diagonals of the 2Fe unit cell. Calculations performed on a possible bicollinear phase showed that such a phase, stable within DFT only for the 11 FeTe compound [12,13], could not be stabilized, so that the calculations always converge to the nonmagnetic phase. This finding is neither surprising nor in contrast with the present understanding of the magnetism in Fe-based compounds: a stable bicollinear phase requires the presence of an additional exchange constant (J_3), coupling next next-nearest-neighbors Fe atoms (i.e., a long-range interaction) that should be larger than J_2, J_2 being the next-nearest-neighbours coupling constant. We point out that FeTe is indeed the only material (among the 11 and 1111) showing a relevant density of states with p-like character on the chalcogen/pnictogen atom at the Fermi level, that could thus support the required long-range magnetic coupling.

The results of our calculations for the pure stoichiometric compounds ($x = 0.0$) are reported in Table I for the most stable phase which results to be the AFM2, for all the pure 42214 compounds. Calculations predict a stripe collinear ground state and thus a possible transition from a tetragonal nonmagnetic high-temperature phase to an orthorhombic antiferromagnetic phase at low temperature, similar to what is observed in most of the other Fe-based families. Low-temperature structural, magnetic, and transport measurements are not available at the moment and thus are highly desirable in order to confirm our predictions.

TABLE I. Calculated values of lattice parameters (a,b,c), As height (h_{As}), equilibrium parameters [bulk modulus B_0 and magnetic properties: total energy difference ΔE between AFM2 and nonmagnetic (NM) states, and magnetic moment μ_{Fe}] for the pure 42214 compounds considered.

	Pr	Sm	Gd
a (Å)	4.08	4.01	3.97
b (Å)	4.05	3.98	3.93
c (Å)	30.20	29.68	29.31
h_{As} (Å)	1.26	1.29	1.31
V (Å^3)	499.03	473.69	457.30
B_o (GPa)	73.60	77.91	80.40
ΔE (meV/atom)	20.30	16.12	14.10
μ_{Fe} (μ_B)	1.96	1.83	1.74

It is interesting to consider the effect of the RE on the structure, as reported in Table I: moving from Pr to Gd (i.e., reducing the covalent radius R), the RE substitution induces a chemical pressure shrinking the volume, increasing the bulk modulus and raising the As height with respect to the Fe planes, as also observed by experiments.

At the same time, larger As height with respect to Fe planes has been often related with enhanced correlation effects and smaller effective magnetic exchange couplings [14]. Indeed, we find that the structural modifications due to the RE substitution induce a decreasing of the Fe magnetic moment and lower the magnetic stability: in fact, the energy difference between the AFM2 and the nonmagnetic phase decreases of about 21% substituting Pr with Sm and a further 13% switching from Sm to Gd. Similar calculations performed considering the 1111 family (LaOFeAs and PrOFeAs compounds) show a change of about 9% in the total energy across the magnetic transition. Although not being a rule, the new 42214 compounds draw stronger magnetic instabilities, compared to the 1111 family, and therefore they might be good candidates for possible higher superconductivity. We found that a significant comparison with experimental data necessarily implies consideration of the native Te vacancies, as discussed in Sec. VI.

IV. PRESSURE EFFECTS

It is well known that applied pressure constitutes a very powerful tool to investigate material properties; in particular, its influence on the superconducting properties of the materials

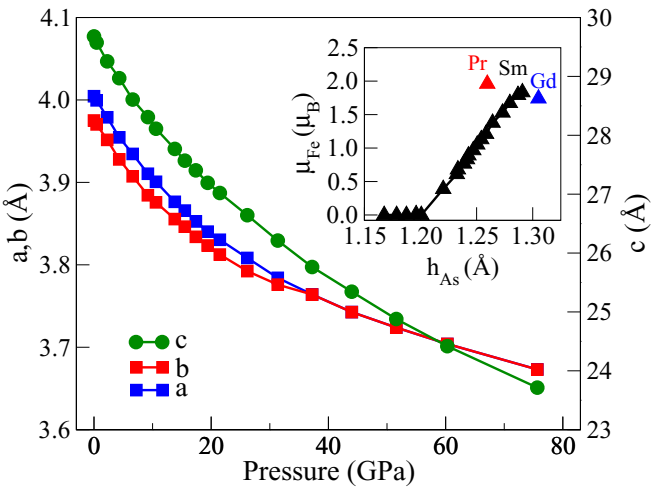

FIG. 2. Structural orthorhombic parameters as a function of pressure and magnetic moment as a function of the As height with respect to the Fe plane (inset) for the pure Sm-based compound (for comparison, equilibrium values of each single pure 42214 compound are also shown).

TABLE II. Structural parameters [lattice parameters (a,b,c), As height (h_{As}), and volume] at the critical pressure values where transition from the orthorhombic to the tetragonal phase occurs in the different 42214 pure compounds.

	Pr	Sm	Gd
a_{crit}, b_{crit} (Å)	3.85	3.76	3.67
c_{crit} (Å)	26.65	25.82	24.50
h_{As} (Å)	1.17	1.20	1.22
V_{crit} (Å^3)	395.00	365.00	330.00
P_{crit} (GPa)	29.80	37.22	57.10

has been often exploited to induce superconductivity or further increase the superconducting transition temperature: as an example, there are many studies on the Fe-based compounds where hydrostatic as well as anisotropic pressure has been shown to greatly affect superconductivity [15–20]. Therefore, in the following we discuss pressure effects on 42214 compounds in order to predict possible structural and magnetic phase transitions and stimulate further experimental studies.

Figure 2 shows how the structural parameters of the pure Sm-based compounds are affected by external hydrostatic pressure; similar results are obtained for the other RE-42214 pure compounds examined: the most important parameters are summarized in Table II for all of them. We notice that calculations predict a transition from the orthorhombic to the tetragonal phase ($a = b$) joined by vanishing of the long-range magnetic order as a function of pressure. This is common to other FeAs-based families as well and has been also found experimentally: the tetragonal nonmagnetic phase is compatible with a short-range magnetic order associated to rapidly fluctuating large local Fe-magnetic moments [21]. The critical pressure values where long-range magnetic order disappears are accessible by nowadays high-pressure experiments, as recently reported for the 122 ($CaFe_2As_2$, $BaFe_2As_2$ [18,19], and KFe_2As_2 [22]). The lattice parameter values at the critical pressure where this transition occurs are shown in Table II; reducing the covalent radius (from Pr to Gd), all the critical parameters decrease except the As height which is seen to increase. This apparently counterintuitive finding supports the effect previously mentioned: due to conservation of the covalent Fe-As bond length, compression (by means of internal chemical pressure or by external hydrostatic pressure) of the (a,b) plane results in the stretching of the As height. Since the As height is often considered to be one of the most effective parameters to control magnetic instabilities and thus superconductivity in the Fe-based family, we now concentrate on this quantity to compare the effects of internal (chemical) versus external pressure. Thus, the question becomes: can we use RE substitution to somehow mimic the effects of applied pressure? To ascertain this issue, we plot in the inset of Fig. 2 the magnetic moment (for the Sm-based compound under pressure, as an example) as a function of the As height (h_{As}) at each pressure value; in the plot we also report the magnetic moments at the equilibrium h_{As}'s of the different RE-42214 compounds considered. It is clear that RE substitution cannot be simply described as a (hydrostatic) pressure effect.

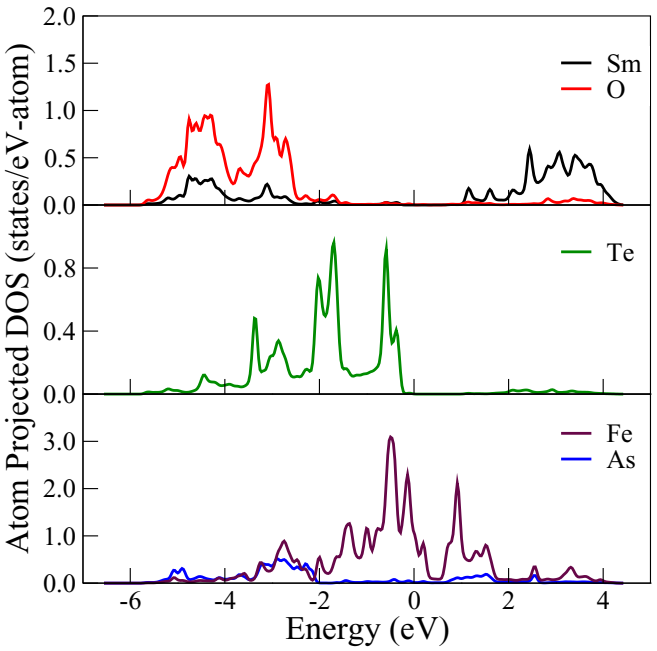

FIG. 3. Atom projected DOS for the pure Sm-based compound in the equilibrium structure: Sm-d states and O-p states (top panel), Te-p states (middle panel), and Fe-d states and As-p states (bottom panel).

However, this provides an additional tool that can be used to tune material properties: changing the RE allows one to explore ranges of h_{As}, and therefore magnetic moment, which are not accessible just applying external pressure [18,19].

V. ELECTRONIC PROPERTIES

In this section we discuss the electronic properties and investigate how different RE atoms and structure affect these properties of 42214 pure compounds. Figure 3 shows the density of states (DOS) projected on each atom type and resolved in orbital contribution for the Sm-based compound, taken as an example. The region close to the Fermi level (E_F), is dominated by Fe d states and As p states forming the Fe-As bond; all the other atoms, namely, RE, O, and Te, contribute very little in this energy region. As a matter of fact, the O p states give rise to fully occupied bonding states localized at high binding energies (from -5 to -1 eV below E_F) hybridized with RE states which have a large unoccupied component at quite higher energies above E_F, marking the ionic character of the bond. Tellurium p states form a dispersed band of about 4 eV energy width below E_F. Therefore, RE-O and Te planes are not hybridized with the states playing an important role at the Fermi level.

The calculated band structure of the compounds for the nonmagnetic tetragonal structure with 2Fe-atoms/cell/layer is reported in Fig. 4 (upper panel) [23]: the states around the Fermi level resemble very closely the prototype band structure shared by most of the Fe-pnictide superconductors. The Fe-$d_{xz,yz}$ bonding states pointing towards the As atoms form hole pockets around the zone center and electron pockets at the zone corner M point (π/a, π/a, 0); the $d_{x^2-y^2}$ are also close

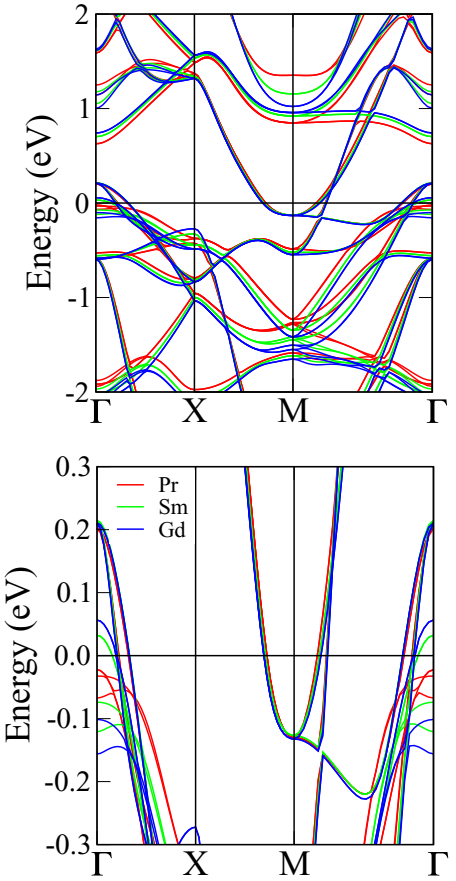

FIG. 4. Band structure of the $RE_4Fe_2As_2TeO_4$, RE = Pr, Sm, and Gd in their respective equilibrium structure in the nonmagnetic state (upper panel); blowup of the same band structure in the energy region closer to the Fermi level (lower panel). Both band structures are shown on the basal plane (see text).

to (crossing or not depending on RE; see below) the Fermi level, while the d_{xy} form bonding/antibonding combinations well below/above the Fermi level (−2.0/1.0 eV). Focusing on the energies close to E_F, Fig. 4 (lower panel) highlights the role of RE, which does not affect the electron hole pockets at M, while it changes quite sensibly the occupation at the zone center. In particular, the $d_{x^2-y^2}$ state at the Γ point is filled in the Pr compound, while it forms hole pockets in Sm and Gd-based compounds [24]. On the contrary, all REs considered show completely filled d_{z^2} states.

This picture is in line with the different structures of the pure 42214 compounds: changing Pr with smaller atoms (Sm and Gd) results in internal pressure effects on the Fe-As planes and a compression of the in-plane bonds. At the M point, where this compression is ineffective, no changes are observed upon substitution of the RE element. In order to better exemplify the RE chemical effect, we plot the band structure of the Pr-based pure compound at its equilibrium phase and at the equilibrium parameters of Sm and Gd compounds (Fig. 5). We note that the shift of $d_{x^2-y^2}$-like states is mainly due to the structural effect (i.e., (a,b)-plane dimensions and h_{As}, as also discussed for 1111 compounds [25]) induced by the different RE atomic sizes: this state is below E_F in the Pr equilibrium structure,

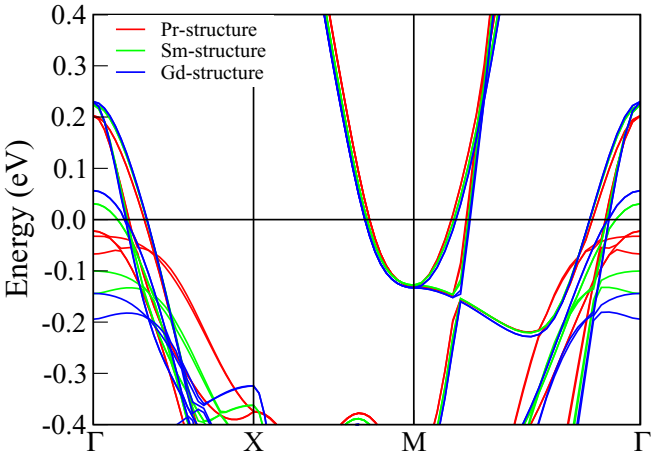

FIG. 5. Comparison of the band structure of $Pr_4Fe_2As_2TeO_4$ at its equilibrium structure (red line) and in the Sm structure (green line) and Gd structure (blue line).

while it is pushed above the Fermi level in the smaller Sm and Gd volumes. Larger differences are also observed in the states at higher binding energy where RE-state hybridization comes into play.

The three-dimensional (3D) Fermi surface (FS) of the Gd compound drawn on the primitive bct cell containing two Fe atoms per cell is shown in Fig. 6 and reveals that, despite the different crystal phase and the additional RE-O and Te planes, the shape of the FS strongly resembles those of 122 (and 1111) compounds: we distinguish three concentric cylinders (holelike) at the zone center, the most internal one having $d_{x^2-y^2}$ character and the two external ones with $d_{xz,yz}$ characters. An additional two cylindrical features exhibiting electronlike character are found at the X corner points.

The cuts of the 3D FS on the basal plane are reported in Fig. 7 (top panels) for all the pure compounds examined. Here, the FS is folded back into the 1Fe unit-cell Brillouin zone, rotated by $\pi/4$ with respect to the 2Fe cell, so that the electron FSs at the corner points are brought into the new X points. This plot would help the interpretation of future ARPES experiments [26–28], as the two inequivalent Fe atoms are seen to only modulate the intensity of the states observed.

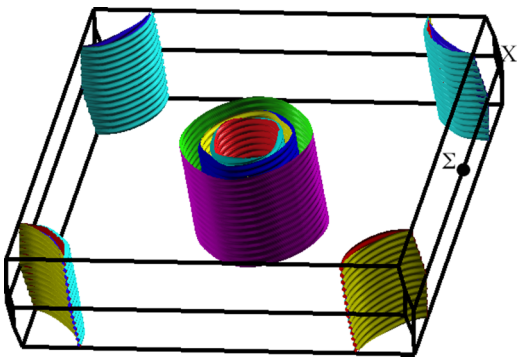

FIG. 6. 3D view of the Γ-centered Fermi surface of the $Gd_4Fe_2As_2TeO_4$ at its equilibrium structure in the 2Fe bct-primitive cell.

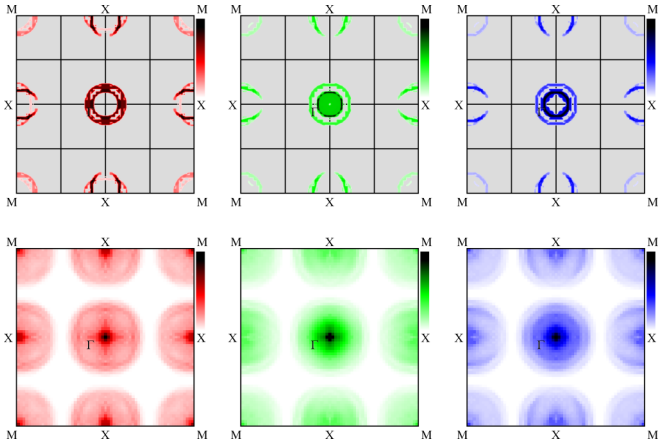

FIG. 7. Fermi surface (top panels) and nesting function (bottom panels) projected on the basal plane of the 1Fe bct unit cell for $RE_4Fe_2As_2TeO_4$ (RE = Pr) (left panels), Sm (center panels), and Gd (right panels) at their respective equilibrium structure. The color intensity is proportional to the value of the nesting function normalized to its value at the zone center.

The Fermi surfaces show similar features in all the compounds considered: two external hole pockets at the Γ point and an internal one which is missing in the Pr compound, and two electron holes at the X points which look almost superimposed in Sm and Gd, while they cross each other in the Pr compound. In fact, the two ellipses surrounding the X points are much closer to degeneracy in Sm and Gd than in Pr: we recall here that degeneracy of the electron pockets has been put forward by some theories to explain the role of F dopant in 1111 compounds, as it is considered to be a fingerprint of interorbital fluctuations that, weakening magnetic interactions, may favor onset of superconductivity [29].

In order to complete the scenario of the electronic properties, we address the possible origin of the superconducting instability. In a first-principles theory of spin-mediated effective interaction [30], a fundamental role is played by the spin susceptibility (χ_{zz}) which determines the strength of the pairing field. A determination of the effective interaction and of the renormalized χ_{zz} is beyond the scope of the present work and is left to a dedicated study; however, useful information on the origin of the superconducting instability can be obtained from the calculation of the bare one-electron susceptibility, $\chi_0(\vec{q},\omega) = \sum_k \frac{[f(\epsilon_{\vec{k}+\vec{q}})-f(\epsilon_{\vec{k}})]}{(\epsilon_{\vec{k}+\vec{q}}-\epsilon_{\vec{k}}-\omega-i\delta)}$ where $\epsilon_{\vec{k}}$ is the one-electron energy, f is the Fermi function, and matrix elements are neglected. To the superconducting problem, the relevant quantity is the so-called nesting function defined as $\chi_0(\vec{q},\omega)/\omega$ for $\omega \to 0$. The nesting function is reported in Fig. 7 (bottom panels) for all the pure 42214 materials considered in the Γ-X-M plane of the 1Fe Brillouin zone. The plots show rather large nesting function values for $\vec{k}$ vectors close to X, marking the calculated instability towards the AFM2 stripe phase, and to a lesser extent to M. The general feature of the nesting function suggests that the superconducting instability in 42214 compounds can be traced back to spin-fluctuation pairing originated by the nesting of the hole and electron pocket at the AFM2 wave vector, similarly to other Fe-based superconducting families.

In conclusion, our study on the electronic properties of the pure compounds shows that (i) the 42214 compounds share their main bonding features with the other Fe-pnictide superconductors; (ii) the layered structure of these compounds allows for additional degrees of freedom that could be used to properly tune their electronic properties; (iii) the magnetic state is found to be more stable for the larger-size RE (namely, Pr) than for the smaller ones; and (iv) similarly to other pnictides, spin fluctuation at $\vec{q} = (\pi/a,\pi/a,0)$ can be at the origin of the pairing mechanism.

VI. Te VACANCIES

An important difference between the structural model we discussed in the previous sections and the real synthesized 42214 compounds is the presence of Te vacancies. Available experimental results give information regarding the Te-vacancies concentration only and not on their spatial distribution. Furthermore, very little is known on how Te content affects the structural, magnetic, electronic, and possibly superconducting properties, due to the difficulties in realizing pure stoichiometric compounds.

As a first step forward to understand the structural implications of the Te-vacancies presence, we considered a $(\sqrt{2}a \times \sqrt{2}b)$ supercell for all the compounds at fixed Te content (50%, 75%, and 100%); from these optimized structures in the stable AFM2 we interpolate the theoretical Te concentrations to extract the structural parameters at the corresponding experimental Te content (namely, 88%, 92%, and 90% for Pr, Sm, and Gd, respectively). In Fig. 8 we compare the interpolated parameters as a function of the RE covalent radius with experiments. The experimental trend is well reproduced by the theoretical results for all the considered parameters, as a function of the covalent radius R; somewhat larger discrepancies (up to 5%) are found comparing the value

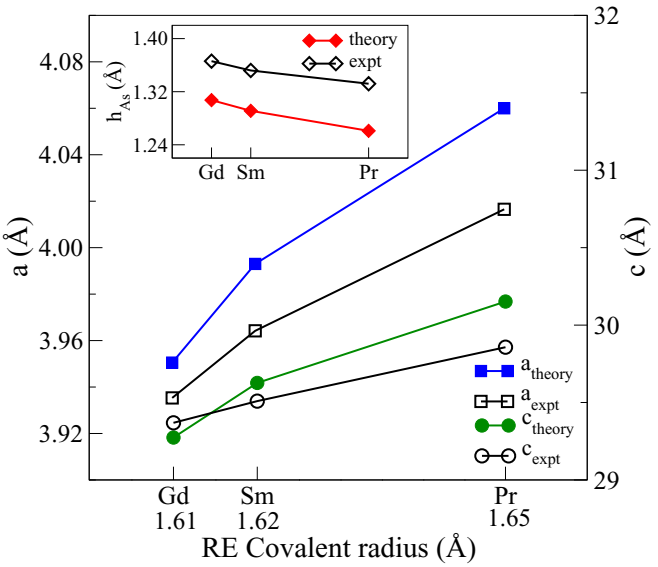

FIG. 8. Comparison between theoretical and experimental values of the main structural parameters as a function of the covalent radius of the RE element. The inset shows the dependency on the RE of the As height with respect to the Fe planes.

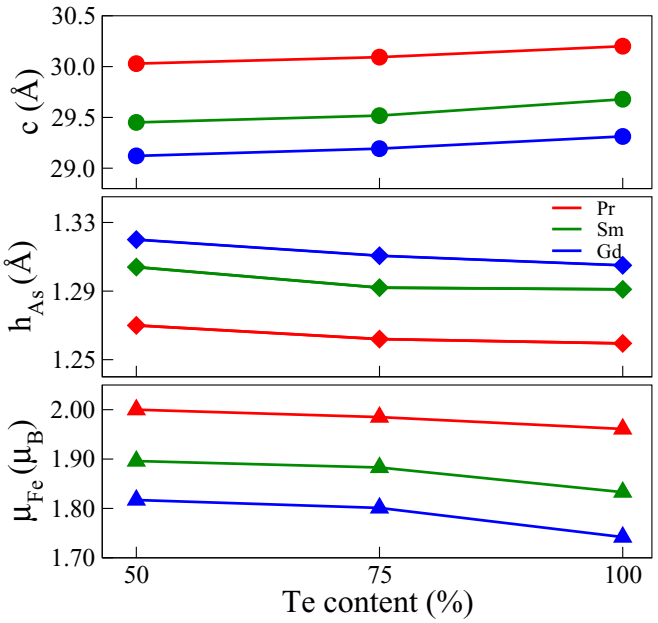

FIG. 9. c-lattice parameter (top panel), h_{As} (central panel), and magnetic moment μ_{Fe} (bottom panel), as a function of Te content.

related to the As height with respect to the Fe planes. However, as already found for most of the Fe-based compounds, this is related to the accuracy of DFT-GGA since this parameter is connected to possible spin fluctuation [14]. Figure 9 reports the calculated values of the parameters most affected by these defects, namely, the c lattice parameter, the h_{As}, and the magnetic moment as a function of Te content. These results confirm the major role played by rare-earth atoms in determining the main structural parameters as Te vacancies. Even at rather large concentrations, they only marginally affect the structure: the c parameter shows a rather small decrease (up to 1%) even at large Te-vacancies concentration (50%). On the other hand, the h_{As} has the opposite behavior: it slowly increases as the Te content decreases. The magnetic moment is once more found to be correlated with the As height and is shown to increase as well. However, despite the increase of the magnetic moment, the stability of the AFM2 magnetic phase with respect to the nonmagnetic phase (not shown) decreases as the Te content is lowered. This is a nontrivial effect which, together with the h_{As} behavior, is seen to favor spin-fluctuations. These issues, however, go beyond the goal of the present study and will be the object of further investigations. However, the present results clearly point out that Te content constitutes an additional tool that could be used to further modify the structure allowing a fine tuning of those parameters that are thought to play a key role for superconductivity.

VII. CONCLUSIONS

To summarize, we presented a detailed and systematic study of the $RE_4Fe_2As_2Te_{1-x}O_4$ (RE = Pr, Sm, and Gd). Our calculations provide insights into the physics of this new compound family and help in understanding many of their structural, magnetic, and electronic properties. In particular, we find that (i) different rare earths induce different internal pressure effects; (ii) similar to other iron-based pnictide superconductors, the 42214 compounds have an orthorhombic, antiferromagnetic-stripe low-temperature phase (although not yet experimentally observed); (iii) smaller size RE ions contribute to increase the magnetic instability through a combined structural and electronic effect (higher As height, lower energy difference between nonmagnetic and AFM2 state, lower nesting function); and (iv) carefully considering the presence of native Te vacancies improves the agreement between theory and experiments, bringing the differences between measured and calculated lattice parameters to less than 1%.

In the large family of Fe-based superconductors, $RE_4Fe_2As_2Te_{1-x}O_4$ compounds show many structural and chemical peculiarities which can be tailored to optimize material properties. Many other aspects, such as combined doping on Te and O sites and possibly on As sites should be investigated to explore the full phase diagram of this new class of materials in order to complete the scenario and ascertain which are the main mechanisms that drive the sought-after material properties.

ACKNOWLEDGMENTS

This work was supported by SUPER-IRON (EU-FP7 grant), PRIN-2012 (IT-MIUR grant), and HPC ISCRA-B and ISCRA-C grants at Cineca HPC center. F.B. acknowledges the ERASMUS program at Università degli studi dell'Aquila for financial support during the period at MPI.

[1] J. K. Glasbrenner, I. I. Mazin, Harald O. Jeschke, P. J. Hirschfeld, and Roser Valenti, Nat. Phys. **11**, 953 (2015).
[2] G. R. Stewart, Rev. Mod. Phys. **83**, 1589 (2011).
[3] S. Katrych, K. Rogacki, A. Pisoni, S. Bosma, S. Weyeneth, R. Gaal, N. D. Zhigadlo, J. Karpinski, and L. Forró, Phys. Rev. B **87**, 180508(R) (2013).
[4] S. Katrych, A. Pisoni, S. Bosma, S. Weyeneth, N. D. Zhigadlo, R. Gaal, J. Karpinski, and L. Forró, Phys. Rev. B **89**, 024518 (2014).
[5] P. J. W. Moll, X. Zhu, P. Cheng, H-H. Wen, and B. Batlogg, Nat. Phys. **10**, 644 (2014).
[6] G. Kresse and J. Furthmuller, Phys. Rev. B **54**, 11169 (1996).
[7] G. Kresse and J. Furthmuller, Comput. Mater. Sci. **6**, 15 (1996).
[8] J. P. Perdew, K. Burke, and M. Ernzerhof, Phys. Rev. Lett. **77**, 3865 (1996).
[9] P. E. Blochl, Phys. Rev. B **50**, 17953 (1994).
[10] H. J. Monkhorst and J. D. Pack, Phys. Rev. B **13**, 5188 (1976).
[11] Y. Mizuguchi, Y. Hara, K. Deguchi, S. Tsuda, T. Yamaguchi, K. Takeda, H. Kotegawa, H. Tou, and Y. Takano, Supercond. Sci. Technol. **23**, 054013 (2010).
[12] M. Monni, F. Bernardini, G. Profeta, and S. Massidda, Phys. Rev. B **87**, 094516 (2013).

[13] C. Tresca, F. Ricci, and G. Profeta, 2D Mater. **2**, 015001 (2014).
[14] C. Zhang, L. W. Harriger, Z. Yin, W. Lv, M. Wang, G. Tan, Y. Song, D. L. Abernathy, W. Tian, T. Egami, K. Haule, G. Kotliar, and P. Dai, Phys. Rev. Lett. **112**, 217202 (2014).
[15] E. Colombier, S. L. Budko, N. Ni, and P. C. Canfield, Phys. Rev. B **79**, 224518 (2009).
[16] W. J. Duncan, O. P. Welzel, C. Harrison, X. F. Wang, X. H. Chen, F. M. Grosche, and P. G. Niklowitz, J. Phys.: Condens. Matter **22**, 052201 (2010).
[17] T. Yamazaki, N. Takeshita, R. Kobayashi, H. Fukazawa, Y. Kohori, K. Kihou, C. H. Lee, H. Kito, A. Iyo, and H. Eisaki, Phys. Rev. B **81**, 224511 (2010).
[18] N. Colonna, G. Profeta, and A. Continenza, Phys. Rev. B **83**, 224526 (2011).
[19] N. Colonna, G. Profeta, A. Continenza, and S. Massidda, Phys. Rev. B **83**, 094529 (2011).
[20] J. Zhao, H. Liu, L. Ehm, D. Dong, Z. Chen, Q. Liu, W. Hu, N. Wang, and C. Jin, Inorg. Chem. **52**, 8067 (2013).
[21] P. Vilmercati, A. Fedorov, F. Bondino, F. Offi, G. Panaccione, P. Lacovig, L. Simonelli, M. A. McGuire, A. S. M. Sefat, D. Mandrus, B. C. Sales, T. Egami, W. Ku, and N. Mannella, Phys. Rev. B **85**, 220503 (2012).
[22] J-J. Ying, L-Y. Tang, V. V. Struzhkin, H-K. Mao, A. G. Gavriliuk, A-F. Wang, X-H. Chen, and X-J. Chen, arXiv:1501.00330.
[23] Note that in the tetragonal unit cell (containing two FeAs planes) each band is exactly double degenerate due to perfect folding along the Γ-Z.
[24] We point out that considering the experimental lattice constants and internal z_{As} parameter the band structures of Sm and Gd compounds are not qualitatively affected, while for the Pr compound, where the $d_{x^2-y^2}$ state appears just above E_F at the Γ point considering the theoretical optimized values, results occupied considering the experimental structure.
[25] M. Monni, F. Bernardini, G. Profeta, A. Sanna, S. Sharma, J. K. Dewhurst, C. Bersier, A. Continenza, E. K. U. Gross, and S. Massidda, Phys. Rev. B **81**, 104503 (2010).
[26] V. Brouet, M. F. Jensen, P.-H. Lin, A. Taleb-Ibrahimi, P. Le Fèvre, F. Bertran, C.-H. Lin, W. Ku, A. Forget, and D. Colson, Phys. Rev. B **86**, 075123 (2012).
[27] V. Brouet, P.-H. Lin, Y. Texier, J. Bobroff, A. Taleb-Ibrahimi, P. Le Fèvre, F. Bertran, M. Casula, P. Werner, S. Biermann, F. Rullier-Albenque, A. Forget, and D. Colson, Phys. Rev. Lett. **110**, 167002 (2013).
[28] L. Moreschini, P. H. Lin, C. H. Lin, W. Ku, D. Innocenti, Y. J. Chang, A. L. Walter, K. S. Kim, V. Brouet, K. W. Yeh, M. K. Wu, E. Rotenberg, A. Bostwick, and M. Grioni, Phys. Rev. Lett. **112**, 087602 (2014).
[29] Z. Hai-Jun, X. Gang, D. Xi, and F. Zhong, Chin. Phys. Lett. **26**, 017401 (2009).
[30] F. Essenberger, A. Sanna, A. Linscheid, F. Tandetzky, G. Profeta, P. Cudazzo, and E. K. U. Gross, Phys. Rev. B **90**, 214504 (2014).